4ICEGE Thessaloniki-GREECE 2007

4th International Conference on
Earthquake Geotechnical Engineering
June 25-28, 2007
Paper No. 1207

NUMERICAL SIMULATION OF LIQUEFACTION INDUCED LATERAL SPREADING USING SMOOTHED PARTICLE HYDRODYNAMIC

Mounir NAILI [1], Takashi MATSUSHIMA[2], Yasuo YAMADA [3]

ABSTRACT

This paper introduces a Lagrangian mesh-free particle method using Smoothed Particle Hydrodynamics (SPH) to assess the liquefaction induced lateral ground displacement. By assuming the liquefied soil to behave as a viscoplastic fluid during the course of the shaking and using the concept of fluid dynamics, the soil is modelled using a Bingham type constitutive model. The stress-dilatancy behaviour of the soil is represented through a bilinear phenomenological constitutive model relating the yield viscosity to the shear strain.
The results of 1g shaking table experiment performed by (Hamada et al., 1994) to examine the mechanism of the liquefaction-induced lateral spreading after the cease of the shaking are used to validate the proposed method.
The simulation results show that the observed shape of the free surface during the experiment is reproduced with an acceptable accuracy. The simulated maximum ground displacements are consistent with experimental results. However, the maximum amplitude of the time history of the ground flow displacement simulated at three elevations in the middle of the soil box is 1.5 to 2.5 times the observed results.
It is worth to mention that this study represents a contribution to analyze the liquefaction induced lateral ground displacement using a Lagrangian meshfree particle method. It constitutes a promising tool able to handle large displacement and to track free surface shape.

Keywords: Liquefaction, lateral ground displacement, apparent viscosity, Bingham model, SPH

INTRODUCTION

Liquefaction induced lateral ground failure have caused extensive damage to pile foundations of buildings and bridges, embankments, river dikes, pipelines, lifeline system and waterfront structures during large earthquakes. For instance, the soil liquefaction during the 1995 Hyogo-ken Nanbu earthquake, caused widespread damage on reclaimed land and induced large ground displacements in the horizontal direction, resulting in distress to buried lifelines and piles foundations of buildings and bridge piers along the Kobe shoreline (e.g. Hamada et al., 1996). In order to protect these structures and to ensure their stability and serviceability during and after the earthquake shaking, the assessment of the likelihood induced permanent displacement and lateral spreading load is a matter of great concern in seismic proof design.

[1] Postdoctoral research fellow, Earthquake Disaster Prevention Research Group, Public Works Research Institute, Japan, Email: naili55@pwri.go.jp
[2] Associate Professor, Department of Engineering Mechanics and Energy, Graduate School of System and Information Engineering, University of Tsukuba, Japan, Email: tmatsu@kz.tsukuba.ac.jp
[3] Professor, Department of Engineering Mechanics and Energy, Graduate School of System and Information Engineering, University of Tsukuba, Japan, Email: yamada@kz.tsukuba.ac.jp

A variety of numerical methods to predict the liquefaction induced lateral ground displacements exist in the literature. They rely on our understanding of the mechanical behaviour of the liquefied soil during the shaking. For instance, undrained monotonic shear tests, shaking table and centrifuge experiments have revealed that, the liquefied soil behave either as a solid or a viscous fluid during the course of the loading (e.g. Kawakami et al., 1994; Yasuda et al., 1995; Towhata, 2002).

Assuming the liquefied soil to behave with a reduced stiffness after the liquefaction, a two stages finite element analysis to assess the permanent ground displacement has been formulated (e.g. Yasuda et al., 1992). Similarly, considering the liquefied soil as a visco-elastic material, a FEM procedure based on the adaptive mesh technique has been proposed (e.g. Ayden, 1995). Assuming the liquefied soil as a Bingham fluid, Uzuoka used the volume of fluid method to predict both the flow process and lateral spreading load (e.g. Uzuoka, 1998). Using the principal of the minimum potential energy and considering the soil to behave as a viscous fluid, a 2D FEM approach based on the updated Lagrangian method has been implemented (e.g. Tamate and Towhata, 1999).

Because induced displacements are large as reported from post-earthquake observations, grid based numerical methods such as FEM face sometimes mesh distortion problem, as it is difficult to handle large deformation. In this case, special treatment of the mesh is necessary to overcome numerical instability, which may lead to time-consuming computation. Similarly, VOF based on a staggered mesh needs special treatment to track moving boundary and interface.

This paper introduces a SPH method in the framework of fluid dynamics to assess ground displacements induced by lateral spreading. The behaviour of the soil is represented by means of Bingham fluid model, while the recovery of rigidity is taken into account through a bilinear phenomenological constitutive model relating the yield viscosity to the shear strain. The capability of the method to reproduce free surface shape, time history of ground flow displacements and shear strain rate is investigated using the results of 1g shaking table experiment to examine the mechanism of the liquefaction-induced lateral spreading after the cease of the shaking (e.g. Hamada et al., 1994)

SPH FORMALISM

The Smoothed Particle Hydrodynamics (SPH) is a pure Lagrangian meshfree particle method, where the continuous media is discretisized by a set of equi-spaced unconnected particles that follow its motion and advect its contact discontinuities. The particles carry the domain's quantities such as the mass, the velocity vector, etc. and thus forming not only the geometrical domain but also the computational framework. For its formulation, one may refer to the original paper (e.g. Gingold and Monaghan, 1977).

To extend the SPH to model the liquefaction induced lateral ground displacement, the liquefied soil is assumed to behave with a combined characteristic of fluid and solid during the course of the shaking. In this respect, a simple Bingham type model represents the viscoplastic properties of the liquefied soil. Similarly, to take into account the stress-dilatancy behaviour, a simple bilinear phenomenological constitutive relationship relates the yield viscosity and the critical shear strain.

Governing equations

The motion of an incompressible, uniform density fluid is governed by the Navier-Stokes equation expressed by the following equation:

$$\frac{Dv^{\alpha}}{Dt} = -\frac{1}{\rho}\frac{\partial p}{\partial x^{\alpha}} + \nu \frac{\partial}{\partial x^{\beta}}\left(\frac{\partial v^{\alpha}}{\partial x^{\beta}}\right) + g^{\alpha} \qquad (1)$$

In which, $\mathbf{v}$: the velocity vector, ρ : the density, g : the acceleration of gravity, $\nu = \mu / \rho$: the kinetic viscosity, μ : dynamic viscosity *and* $\alpha\beta$: the coordinate system.

SPH formalism

In SPH, the estimation of any physical property is achieved by interpolating from a set of disordered particles by means of a kernel function, which represents a weighted sum over neighbouring particles within an area defined by the smoothing length. This can be expressed as:

$$f(\mathbf{x}) = \int_{\Omega} f(\mathbf{x}')W(\mathbf{x}-\mathbf{x}', h)d\mathbf{x}' \approx \sum_{j=1}^{N} \frac{m_j}{\rho_j} f(\mathbf{x}_j)W(\mathbf{x}-\mathbf{x}_j, h) \tag{2}$$

In which, h: smoothing length defining the influence domain and $W(\mathbf{x}-\mathbf{x}', h)$: kernel function which should satisfy the following normalization condition:

$$\int_{\Omega} W(\mathbf{x}-\mathbf{x}', h)d\mathbf{x}' = 1 \tag{3}$$

Similarly, the derivative of the kernel function is expressed as:

$$\nabla f(\mathbf{x}) \approx \sum_{j=1}^{N} \frac{m_j}{\rho_j} f(\mathbf{x}_j)\nabla W(\mathbf{x}-\mathbf{x}_j, h) \tag{4}$$

Using Eq.(2) and Eq.(4), the SPH expression for the Navier-Stokes Eq.(1) is obtained as follow:

$$\frac{Dv_i^{\alpha}}{Dt} = -\sum_{j=1}^{N} m_j \left(\frac{p_i}{\rho_i^2} + \frac{p_j}{\rho_j^2}\right)\frac{\partial W_{ij}}{\partial x_i^{\alpha}} + \sum_{j=1}^{N} m_j \left(\frac{\mu_i \varepsilon_i^{\alpha\beta}}{\rho_i^2} + \frac{\mu_j \varepsilon_j^{\alpha\beta}}{\rho_j^2}\right)\frac{\partial W_{ij}}{\partial x_i^{\beta}} + g^{\alpha} \tag{5}$$

At this stage, the SPH is unable to model truly an incompressible fluid as the flow is driven by local density fluctuation. This constraint is resolved by solving for the flow of a nearly incompressible fluid using an equation of state and enforcing the density fluctuation difference to be less than 1%, i.e. $\Delta\rho \leq 0.01$. In this study, the pressure term p proposed by Gingold and Monaghan (1977) is used as:

$$p = B\left(\left(\frac{\rho}{\rho_0}\right)^{\gamma} - 1\right) \tag{6}$$

Where γ : a constant equals to 7 in this study, ρ_0 : initial density, B : a parameter that sets a limit for the density fluctuation difference.

The SPH formulation as introduced here is only valid for a Newtonian fluid and thus has to be modified to include the case of a liquefied soil, which is represented herein by a viscoplastic model in term of a Bingham constitutive law.

SPH formulation for a non- Newtonian fluid

The general equation of the momentum in Eq. (5) is used to model a Non-Newtonian fluid, where an equivalent viscosity is inserted in the SPH approximation of the viscous forces as follow:

A Bingham type fluid has the following shear stress-shear strain rate relationship.

$$\tau = \tau_{\min} + \mu_B \dot{\gamma} \tag{7}$$

Where τ_{min} represents the minimum undrained shear strength and μ_B its viscosity
If we define an equivalent viscosity in the form of Eq. (8), a non Newtonian fluid can be modelled as a Newtonian type fluid.

$$\mu_{eff} = \mu_B + \frac{\tau_{\min}}{\dot{\gamma}} \tag{8}$$

Where $\dot{\gamma}$ is given by the second invariant of the deviatoric strain rate tensor.

$$\dot{\gamma} = \sqrt{\frac{1}{2} \dot{e}_{\alpha\beta} \dot{e}_{\alpha\beta}} \tag{9}$$

NUMERICAL SIMULATION

The ability of the SPH method to simulate the liquefaction-induced lateral spreading is investigated using the results of the experiments conducted by Hamada (e.g. Hamada et al., 1994).
To examine the mechanism of the liquefaction induced lateral spreading after the end of the shaking, the authors performed a series of 1g shaking table experiments, in which a model ground with an initial plane surface was constructed in a rigid soil box as shown in Figure 1. The box was vibrated in the lateral direction with a sinusoidal wave acceleration of 100 cm/s^2 until a total liquefaction occurs, and then lifted with a specific gradient using a hydraulic jack. During the experiment, the final shape of the free surface was continuously monitored and the time history of the induced displacements was measured at three different depths in the middle of the soil box. Several tests were performed by considering an initial relative density of the soil between 23% and 61%, and an inclination of the soil box equals to 2.1% and 4.2% respectively. The numerical simulation attempts herein to simulate the case in which the relative density of the soil is 41% and the soil box inclination is 4.2%.

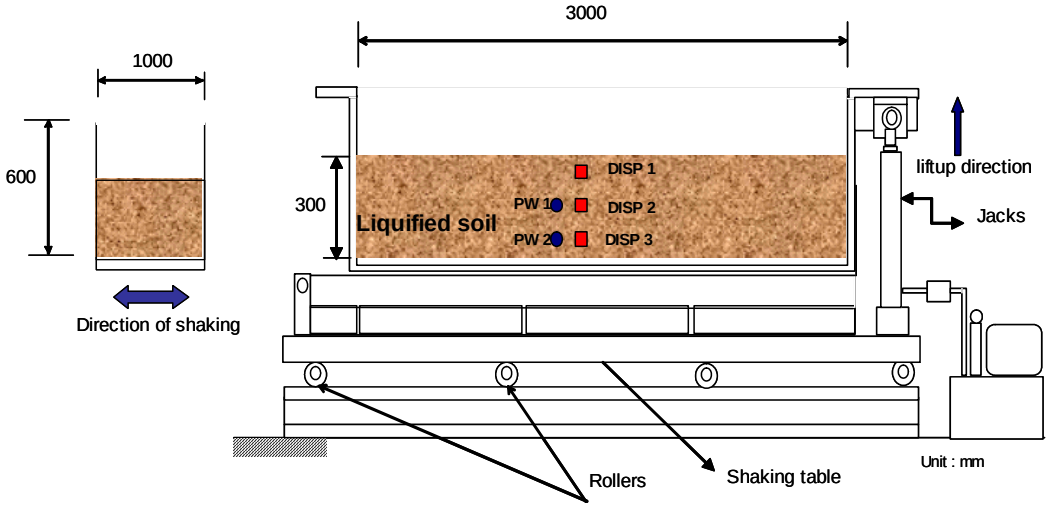

Figure 1.Experimental setup after Hamada et al., 1994

Numerical setup

The required input parameters used for the simulations are of two types; those related to the viscoplastic Bingham model, and those related to the stress dilatancy model or the recovery of rigidity.

Two parameters specify the viscoplastic Bingham model; i.e. the yield viscosity of the liquefied soil and the minimum undrained shear strength. Similarly, a relationship between the yield viscosity and the critical shear strain defines the stress dilatancy model as shown in Figure 2. It is expressed with a bilinear curve defined by Equation (10).

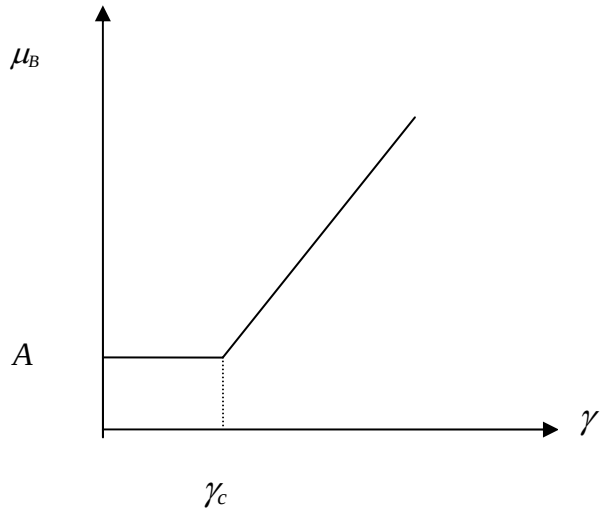

Figure 2. Proposed constitutive model for the recovery of the rigidity

$$\begin{aligned} \mu_B &= A && \text{if } \gamma \le \gamma_c \\ \mu_B &= (B\gamma + C) && \text{if } \gamma > \gamma_c \end{aligned} \tag{10}$$

Table 1 bellow summarizes the input parameters used for the numerical simulation. In this table, R represents the ratio between the minimum undrained shear strength and the confining pressure. According to the experimental results, the soil started flowing when the soil box reached an inclination of 2%. Accordingly, R is set to 0.02 during the simulation. The critical shear strain $\gamma_{c,}$ takes the value of 10% based on the experimental results (e.g. Hamada and Wakamatsu, 1998).

Table 1. Numerical parameters

Model dimensions (m)	3 x 0.3
Number of particles	150 x 15
Initial spacing (m)	0.02
Density of particles (kg/m^3)	1800
Yield viscosity A or μ_B (Pa·s)	0.1
γ_c	10%
R	0.02
Time increment (s)	10^{-4}
Sound speed (m/s)	50

Simulation cases

There are no established rules on how to select a suitable set of parameters for the stress dilatancy constitutive model, as it is strictly based on a phenomenological concept rather than a physical concept. In this respect, the related parameters are selected to obtain a best fitting against experimental results. Accordingly, two set of parameters are chosen to represent the recovery of the rigidity for the

lateral spreading experiment whose parameters are given in Table 2. Besides these cases, and for the purpose of comparison, a preliminary simulation case without recovery of rigidity is undertaken.

Table 2. Simulation cases

	Model 1	Model 2	Model 3
A (μ_B)	0.10	0.10	0.10
B	-	1.1×10^4	1.1×10^5
C	-	-1.1×10^3	-1.1×10^4

Simulation results

This section highlights the simulation results expressed in terms of free surface shape, time history of the ground flow displacement, maximum ground displacement, relationship between the equivalent viscosity and induced shear strain and finally time history of the strain tensor expressed by its second invariant.

Free surface shape

Figure 3 depicts the simulated free surface shape for Model 1 and Mode 2 with respect to the initial and the final observed ground surface. A clear subsidence in the upstream part due to the gravity as well as a heaving in the downstream part due to the volume transfer is clearly seen. The reproduced shape for Model 1 and Model 2 are different from the observed one in the upstream due to an excess flowing. In the downstream part however, Model 2 reproduces the observed free surface with an acceptable accuracy. Furthermore, the central part keeps the same inclination as the observed one in the downstream part while in the upstream region; the curve depicts a slight rotation with respect to the initial ground surface.

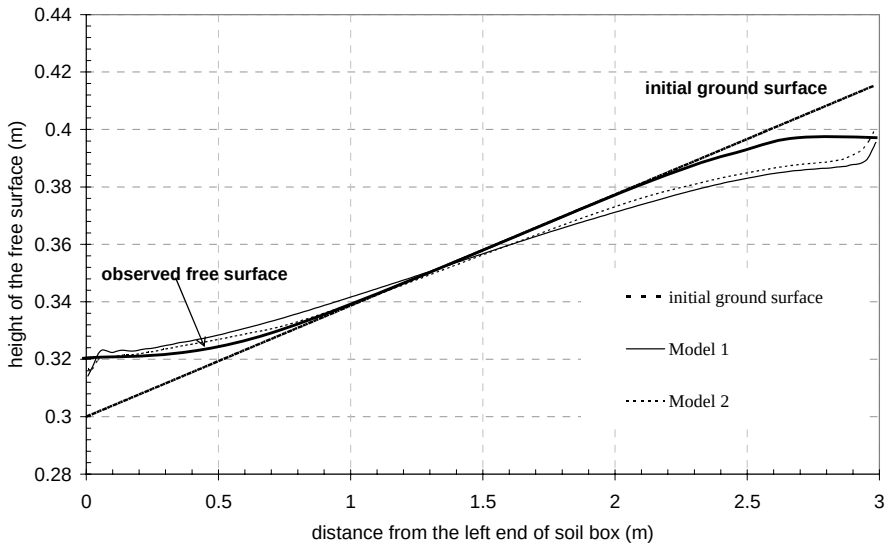

Figure 3. Simulated free surface shape

Time history of the ground flow displacement

Figure 4 shows the time history of the ground flow displacement computed at three elevations at the middle of the soil box for Model 1, Model 2 and Model 3 respectively. The experimental results are also depicted in the same figure. The time history of the ground flow displacement is consistent with the experimental results between 0-2s. From t = 2s, Model 1 shows a continuous flow at all elevation. The magnitude of the simulated displacements lies between 1.75~2.75 times the experimental results.

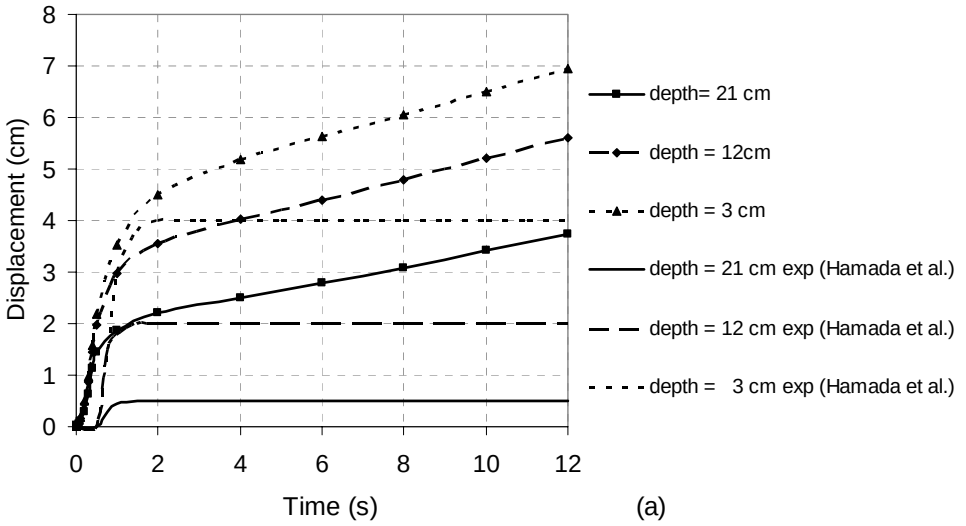

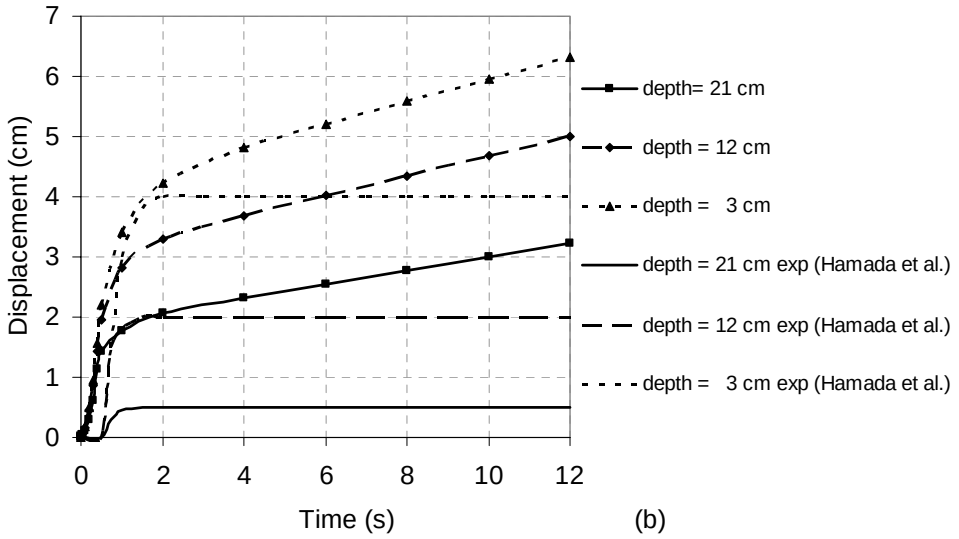

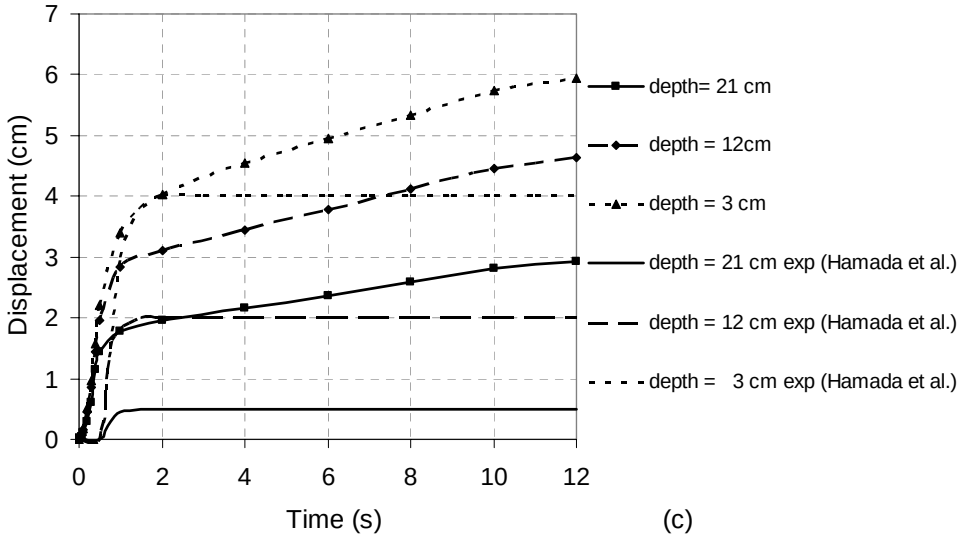

Figure 4. Time history of the ground flow displacement for Model 1, Model 2 and Model 3

By introducing the stress-dilatancy model and increasing the parameters B and C, one distinguishes a slight reduction in terms of magnitude. This implies that the flow has decreased and the liquefied soil regained its rigidity. As for Model 3, the estimated displacement lies between the ranges of 1.5 to 2.5 times the observed one.

A modification of the parameters of the constitutive model for the rigidity recovery was unable to improve the results as expected. This suggests that the proposed phenomenological constitutive model has a limited ability to grasp the whole behaviour of the liquefied soil, causing numerical instability due to the abrupt change from fluid to solid state.

One of the solutions to overcome this instability consists in considering a smaller time step $\Delta t = 10^{-5}$ s. Figure 5 depicts the time history of the ground flow displacement corresponding to Model 3. In this case, the flow tends towards an asymptotic value along the height of the soil model. Further decrease in the time step, was unable to fit the experimental results. Instead, it shows that the bilinear model has some drawbacks in capturing the behaviour of the liquefied soil at the post-liquefaction stage. This is somehow true, as the proposed model does not take into account the dissipation of the pore water pressure.

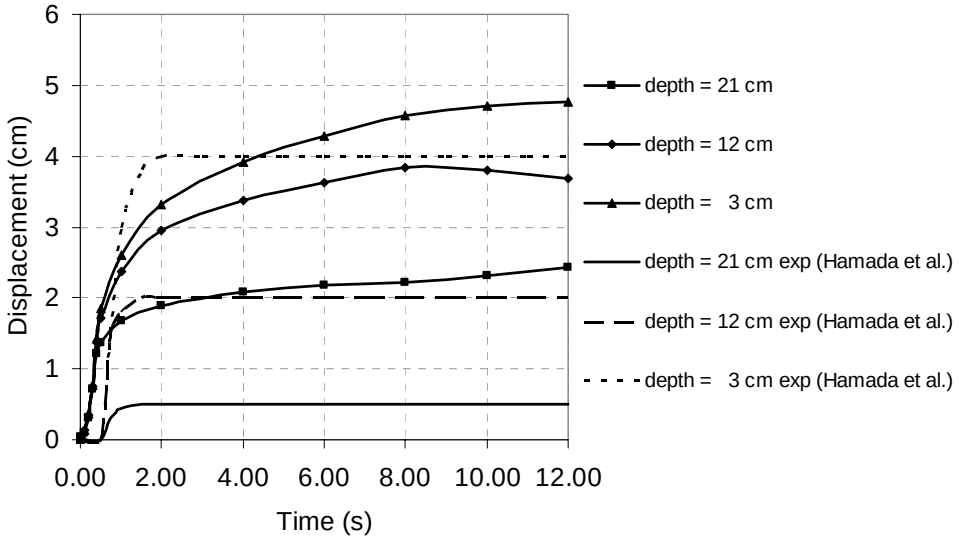

Figure 5. Time history of the ground flow velocity for Model 3 corresponding to $\Delta t = 10^{-5}$ s

Maximum ground displacement

The maximum ground displacements at three elevations computed at three distinct locations were simulated and compared against available experimental results.

Figure 6 shows the distribution of the maximum ground displacement at three elevations at distances equals to 0.5 m, 1.5 m and 2.5 from the left side of the soil box obtained using Model 2 of the recovery of rigidity.

The simulated maximum ground displacements are consistent with the experimental results. At a distance of 2.5 m from the left hand side, the simulated maximum ground displacement is well reproduced at the three respective elevations corresponding to depth h = 3 cm, h = 12 cm and h = 21 cm. However in the central part and at a position equals to 0.5 m from the left side of the soil container, the simulated ground displacements are smaller than the experimental ones.

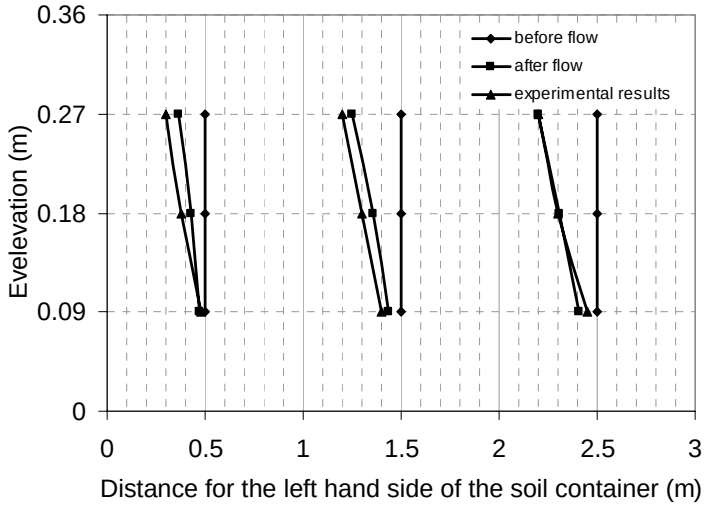

Figure 6. Maximum ground displacement

Relationship between the equivalent viscosity and the induced shear strain rate

Figure 7 shows the relationship between the induced shear strain rate and the equivalent viscosity using Model 2 of the recovery of rigidity. The results are compared to those given by Hamada and Wakamatsu (e.g. Hamada and Wakamastsu, 1998).

The simulated induced shear strain rates at depth h = 21 cm lie within a comparable range as the experimental results. At shallow depth, the computed shear strain rate exhibit smaller value, which implies a limited flow velocity of the liquefied soil.

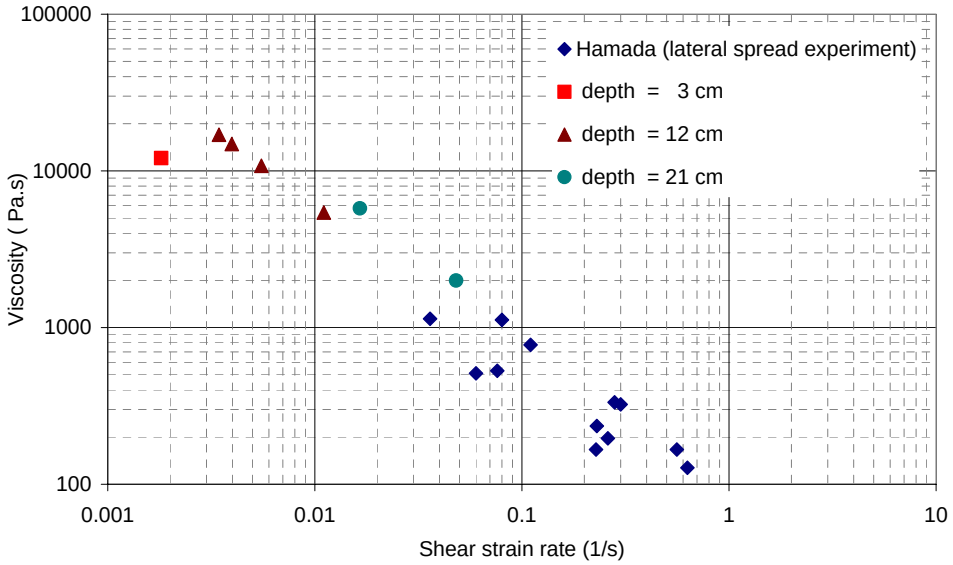

Figure 7. Relationship between the equivalent viscosity and the induced shear strain rate for Model 2

Time history of the induced shear strain

The time history of the induced shear strain expressed in term of second invariant of the strain tensor is computed at three elevations. It is defined by Eq.(11) as follow:

$$\gamma = \sqrt{\frac{1}{2}\varepsilon_{ij}\varepsilon_{ij}} \tag{11}$$

Figure 8 depicts the time history of the second invariant of the strain tensor derived for Model 2 of the recovery of rigidity. At the bottom and at the middle of the soil container, the liquefied soil regains its rigidity, as the induced shear strain is above the critical shear strain.

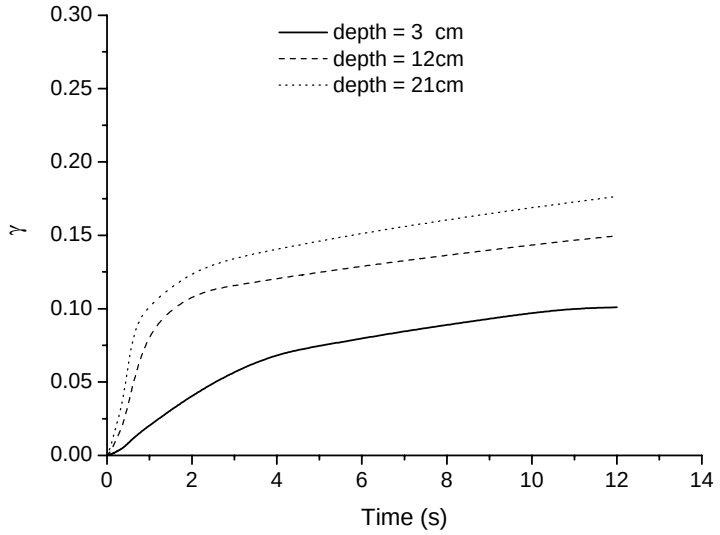

Figure 7. Time history of the second invariant of the strain tensor for Model 2

CONCLUSIONS

This paper introduces a Lagrangian meshfree particle method using Smoothed Particle Hydrodynamics (SPH) to assess the liquefaction induced lateral ground displacement. Assuming the liquefied soil to behave as a viscous fluid during the course of the shaking and using the concept of fluid dynamics, the liquefied soil is modelled by a Bingham type constitutive model. The stress dilatancy behaviour of the soil is considered through a bilinear phenomenological constitutive model relating the yield viscosity to the critical shear strain.

The principal findings are summarised as follow:

1. The shape of the free surface is reproduced with an acceptable accuracy at the downstream part, while the upstream part experienced an excessive flow.
2. The magnitude of the induced displacement is in the range 1.5~2.5 times the experimental results.
3. The simulated maximum ground displacements are consistent with the experimental results.
4. The simulated induced shear strain rates at depth h = 21 cm lie within a comparable range as the experimental results.

It is worthy to mention that this study represents an attempt to analyze the liquefaction induced lateral ground displacement using a Lagrangian meshfree particle method. It is a promising tool able to handle large displacement and track free surface shape. Deriving and implementing a constitutive model, which takes into account the dissipation of the pore water pressure, can improve the simulated results.

REFERENCES

Aydan O, Mechanical and numerical modelling of lateral spreading of liquefied soil. *Proc.1st Int Conf on Earth-Geo Eng, Tokyo* 881-886, 1995.

Gingold, R.A, Monaghan, J.J, Smoothed particle hydrodynamics: Theory and Application to Non-Spherical stars, *Monthly notices of the Royal Astronomical Society*, Vol.181, 375-389, 1977.

Hamada H., Sato H., Kawakami T., A consideration of the mechanism for liquefaction-related large ground displacement. *Proc. 5th US-Japan workshop on Earthquake Resistant Design of Lifeline Facilities and Countermeasures against Soil liquefaction, Technical report NCEER 94-0026, 217-232, 1994.*

Hamada, M., Isoyama, R, Wakamatsu, K., Liquefaction-induced ground displacement and its related damage to lifelines facilities, *Special issue of Soils and Foundations*, 81-97,1996

Hamada, M. and Wakamatsu, K., A study on ground displacement caused by soil liquefaction, *Journal of Geotechnical Engineering, JSCE*, III-43(596),189-208,1998

Kawakami T., Suemasa N., Hamada H., Sato H.,Katada T., Experimental Study on Mechanical Properties of Liquefied Sand. *Proc. 5th US-Japan workshop on Earthquake Resistant Design of Lifeline Facilities and Countermeasures against Soil liquefaction, Technical repor*t *NCEER 94-0026,* 285-299, 1994.

Orense, R, Towhata., Prediction of liquefaction-induced permanent ground displacements: A three dimensional approach, Proc. 4th US-Japan workshop on Earthquake Resistant Design of Lifeline Facilities and Countermeasures against Soil liquefaction, Technical report NCEER 92-0019, 335-349, 1994

Tamate S, Towhata I., Numerical simulation of ground flow caused by seismic liquefaction, *Soil Dynamics and Earthquake Engineering*, 18, 473-485, 1999

Towhata I, Material Properties of Liquefied Sand Undergoing Shaking and Large Deformation, *US-Japan Workshop on Seismic Disaster Mitigation In Urban Area By Geotechnical Engineering* 2002

Uzuoka R., Yashima A.,Kawakami T.,Konrad J.M.,Fluid dynamic based prediction of liquefaction induced lateral spreading. *Computers and Geotechnics*, 22(3/4), 243-282, 1998.

Yasuda S., Nagase H.,Kiku H.,Uchida Y, The mechanism and a simplified procedure for the analysis of permanent ground displacement due to liquefaction. *Soils and Foundations*, 32(1), *149-160,* 1992

Yasuda S., Yoshida N., Masuda T., Nagase H., Mine K., Kiku H.,.Stress-strain relationship of liquefied sand, *Proc.1st Int Conf on Earth-Geo Eng, Tokyo* 811-816, 1995